Shape oscillations: A walk through the phase diagram of strained islands

M. Stoffel,[1,*] A. Rastelli,[1] J. Stangl,[2] T. Merdzhanova,[1] G. Bauer,[2] and O. G. Schmidt[1,3]
[1]*Max-Planck-Institut für Festkörperforschung, Heisenbergstraße 1, 70569 Stuttgart, Germany*
[2]*Institute for Semiconductor Physics, Johannes-Kepler-Universität, A-4040 Linz, Austria*
[3]*Institute for Integrative Nanosciences, IFW Dresden, Helmholtzstrasse 20, 01069 Dresden, Germany*
(Received 15 January 2007; published 14 March 2007)

We observe that the morphology of strained SiGe/Si(001) islands oscillates between shallow and steeper shapes during extensive *in situ* annealing at the growth temperature. We attribute this result to a competition between coarsening and Si-Ge intermixing as paths to strain relaxation. A simple model, in which the equilibrium island shape depends on volume and the average misfit with the substrate, accounts for the observed behavior. Dislocated islands evolve similarly to coherent islands, with no introduction of additional dislocations throughout the annealing.

DOI: 10.1103/PhysRevB.75.113307 PACS number(s): 68.65.Hb, 68.37.Ps, 81.15.Hi

The SiGe/Si(001) material system is widely recognized as a prototype[1–3] for understanding the Stranski-Krastanow (SK) growth in lattice-mismatched semiconductors, which is presently the best way to obtain high quality self-assembled quantum dots. The degree of knowledge reached for the SiGe/Si material system is higher than that for other more complex systems, such as InAs/GaAs (001) (which is more appealing for optoelectronic applications). It was pointed out that several phenomena first observed for the SiGe/Si system are also observed for the InAs/GaAs system.[4] In spite of intense research on SiGe/Si islands over the last decade, there are still new and rather surprising effects, which are continuously reported. One example is the lateral motion of islands, which is driven by asymmetric surface-mediated alloying rather than by bulk interdiffusion.[5]

In this paper, we study yet another surprising effect, which is the observation of shape oscillations during *in situ* annealing of an initially uniform distribution of barn-shaped islands (B).[6,7] We observe that the island shape exhibits an oscillatory behavior, evolving from steep barns to shallower domes (D) and then to pyramids (P), and vice versa. This effect helps us to understand the interplay of two general phenomena, namely "anomalous" coarsening,[8,9] which consists of the growth of steep islands at the expense of shallower islands, and material intermixing.[10–12] Our observations are well accounted for by a simple walk through the phase diagram of SiGe islands, which is constructed from experimental data on island volumes and composition. Finally, we find that dislocated islands, called superdomes (SD), evolve similarly to coherent islands, with no introduction of additional dislocations throughout the annealing.

The samples were grown using solid source molecular beam epitaxy (MBE). After deoxidation and buffer growth, 10 monolayers (ML) of Ge were deposited at 740 °C at a rate of about 0.04 ML/s. The samples were then kept at 740 °C for various times ranging between 1 and 900 min before cooling to room temperature (RT). The surface morphology was investigated by means of atomic force microscopy (AFM) in tapping mode. Some samples were etched in a buffered hydrofluoric acid, hydrogen peroxide, acetic acid (BPA) solution $[HF(1):H_2O_2(2):CH_3COOH(3)]$ or in an ammonium hydroxide, hydrogen peroxide solution $[NH_4OH(1):H_2O_2(1)]$, which are both known to etch selectively $Si_{1-x}Ge_x$ alloys over pure Si.[13,14] The average Ge composition was extracted from x-ray diffraction data measured at the beamline ID10B at the ESRF in Grenoble-France. Reciprocal space maps were recorded around the asymmetric (206) Bragg peak at a wavelength of 0.118 nm. Using the island shapes obtained from AFM, we assume a vertical Ge composition profile varying from bottom to top in a square-root manner, i.e., with a steeper increase at the bottom of the island. We calculated the strain state using the finite element method (FEM) and from the strain distribution, the diffuse x-ray scattering from the elastically relaxed (i.e., coherent) islands is simulated using semi-kinematical scattering theory. The Ge profiles are adjusted to obtain a good agreement between measurement and simulation.[15,16] Since only few SDs are found on the studied samples, and the number of dislocations (and hence the lattice mismatch) varies from SD to SD, they were not included in the x-ray diffraction analysis.

Figure 1 displays AFM scans of samples obtained upon

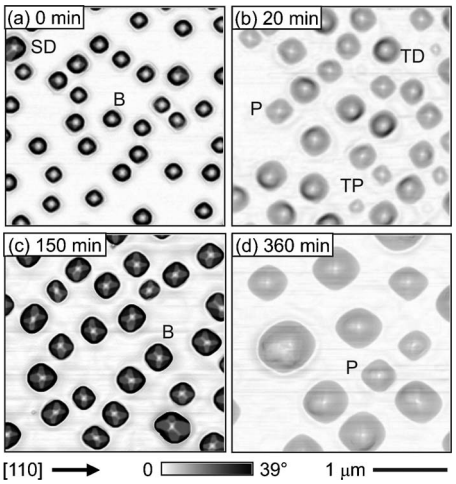

FIG. 1. AFM images of samples obtained upon deposition of 10 ML of Ge at 740 °C (a) and after subsequent *in situ* annealing for 20 min (b), 150 min (c), and 360 min at 740 °C (d). The shading allows steep and shallow facets to be distinguished according to the local surface slope with respect to the (001) plane.

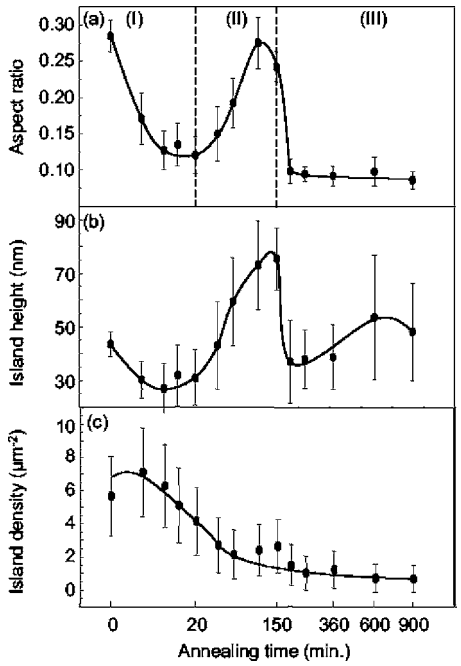

FIG. 2. Evolution of the island aspect ratio (a), height (b), and density (c) with the annealing time. The dashed line in (a) separate different regimes (see text for details).

deposition of 10 ML Ge at 740 °C [Fig. 1(a)], and subsequent *in situ* annealing for 20 min [Fig. 1(b)], 150 min [Fig. 1(c)], and 360 min at 740 °C [Fig. 1(d)]. After deposition of 10 ML Ge at 740 °C, a highly uniform distribution of barns is observed [Fig. 1(a)].[7] A few SDs are also observed. After 20 min of *in situ* annealing [Fig. 1(b)], most of the original barns have transformed back to pyramids or to transitional structures with an intermediate shape between domes and pyramids (transitional domes TDs).[5] Surprisingly, after 150 min of annealing under the same conditions, we observe that pyramids have transformed again into steeper domes and barns [Fig. 1(c)]. Eventually, after 360 min annealing, large {105}-faceted pyramids are found [Fig. 1(d)]. We can thus conclude that the island shape oscillates during annealing.

Figure 2 shows the result of a statistical analysis on the average island aspect ratio [Fig. 2(a)], height [Fig. 2(b)], and density [Fig. 2(c)] as a function of annealing time. Both aspect ratio and height follow an oscillatory behavior with the annealing time. From the evolution of the aspect ratio, we can distinguish three different regimes: (i) For annealing times up to 20 min, the aspect ratio decreases from 0.28 to 0.1 [Fig. 2(a)]. This corresponds to the B-to-D followed by the D-to-P transitions. At the annealing temperatures used in the experiment, two strain-relieving mechanisms can determine the evolution of the island ensemble: anomalous coarsening[8] and/or Si-Ge intermixing. If the former mechanism would be dominant, the largest barns would grow at the expense of smaller ones and the critical volume for dislocation introduction could be exceeded leading to plastic relaxation of the epilayer and appearance of additional SDs. Such an evolution has been reported during *in situ* annealing of InAs/GaAs(001) (Refs. 17 and 18) or PbSe/PbTe(111) quantum dots.[19] In our case, this path is not "chosen," most probably due to the relatively high activation energy barriers for misfit dislocation nucleation.[20] Indeed, for a given epilayer thickness, the energy cost for creating a unit length 60° misfit dislocation is larger for the Ge/Si system than for the InAs/GaAs or CdSe/ZnSe systems.[21] The island ensemble will thus evolve preferentially by SiGe alloying, which leads to shallower morphologies. (ii) For annealing times between 20 and 150 min, the aspect ratio increases from 0.1 to almost the same value measured for the nonannealed sample. We have previously shown that intermixing occurs via lateral island motion, which slows down for sufficiently long annealing times.[5] The simultaneous decrease of the island density [Fig. 2(c)] and the increase of average island height [Fig. 2(b)] suggest that *anomalous coarsening takes over* in this regime. The islands, whose volume exceeds a critical value, undergo a shape transformation from pyramids to TDs and then continue their growth toward steeper domes and barns while smaller islands shrink and disappear.[9] (iii) For annealing times longer than 150 min, the aspect ratio decreases again to almost 0.1 and the barns transform back to domes and then to pyramids, indicating that intermixing becomes dominant again. For annealing times as long as 900 min, we still observe large pyramid islands. We attribute this observation to a progressive slowdown of the processes involved, mainly because of the substantial increase of the lateral size of the islands. This renders it difficult to observe further changes in a reasonable time scale.

The island shape is mainly determined by its size and misfit with the substrate. In order to determine the misfit and composition, we performed x-ray diffraction measurements. Selective wet chemical etching experiments using a $NH_4OH:H_2O_2$ solution were performed to cross check the results. During the regime (I) of the *in situ* annealing, strong Si-Ge alloying is known to occur,[11] leading to island shape changes as soon as the volume drops below a compositional dependent critical volume V_c. If we assume that the misfit ε can be written as $\varepsilon=0.042x$, where x is the Ge content and that the island width scales as ε^{-2},[22–24] V_c can be written as $V_c(x)=V_c(1)/x^6$, where $V_c(1)$ is the critical volume for pure Ge islands. Since neither prepyramids nor domes are usually observed in the growth conditions (low substrate temperature) required to obtain pure Ge islands, $V_c(1)$ should be regarded as a mathematical parameter. We can estimate the critical volume for the prepyramid[1,9] to pyramid transition to be about 4000 nm^3 and the critical volume for the P-to-D transition to be about 2×10^5 nm^3 at 740 °C. The latter values are obtained from the critical size distinguishing shrinking from growing islands in a sample obtained upon deposition of about 5 ML Ge at 740 °C.[9] As the Ge composition profiles obtained from x-ray diffraction are rather flat as a function of island height, we can use the average Ge concentration to evaluate $V_c(1)$, which is 11 nm^3 and 556 nm^3 for the prepyramid to pyramid and the P-to-D transition, respectively. The $V_c(x)$ curves are plotted in Fig. 3(a). We compare our data with the above model for the samples shown in Fig. 1. We measure the mean island volumes from our AFM data. The average Ge content is determined from the vertical Ge profile found from the analysis of finite element simulations of reciprocal space maps. The results are corroborated by wet

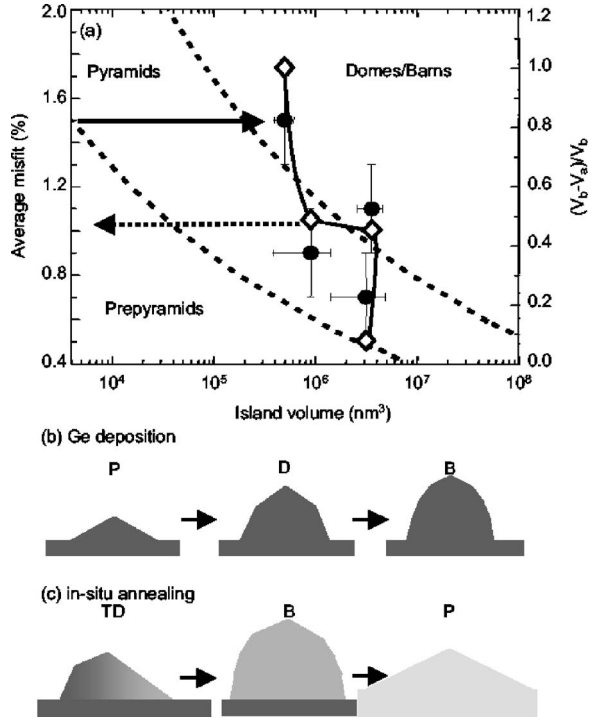

FIG. 3. (a) Island shape as a function of mean volume and average misfit. The dashed curves represent the critical volumes $V_c(x)$ for the prepyramid to pyramid and pyramid to dome transitions and separate the regions in which the equilibrium shape is dome or barn (for simplicity we do not distinguish the two shapes in the figure), pyramid and prepyramid. The solid and dashed arrows show the schematic evolution of growing and shrinking islands, respectively. The solid line shows the pathway followed during post growth annealing. The quantity $(V_b-V_a)/V_b$ (see text for the definition) is shown as open symbols. (b) Schematic of the island shape evolution during growth. The islands evolve from pyramids to domes and finally to steeper barns. (c) Schematic of the island shape evolution during *in situ* annealing. The gray level is related to the island composition.

chemical etching experiments. We first determine the mean island volumes prior to (V_b) and after 210 min etching (V_a) in a $NH_4OH:H_2O_2$ solution. Since this solution etches preferentially Ge over Si, the quantity $(V_b-V_a)/V_b$ gives a rough measure of the Ge content. Figure 3 summarizes our results showing the islands shape as a function of their volume and average Ge composition. Both x-ray [full symbols in Fig. 3(a)] and etching results [open symbols in Fig. 3(a)] follow the same trend. The Ge composition, which is an average over the assumed composition profile, is given with an error bar due to the rather large size distribution of the islands. During growth [Fig. 3(b)], at approximately constant composition, the islands evolve from prepyramids to pyramids and eventually to larger domes and barns following the solid line arrow. When annealing sets in [Fig. 3(c)], the islands move laterally while becoming larger and more dilute. Thus, they will cross the critical volume curve and start to evolve to their precursor shape. For longer annealing times, anomalous coarsening takes over: The larger islands increase their volume, thus being able to cross again the critical volume curve and to evolve to steeper morphologies, while smaller islands shrink and disappear[9] [see dashed line arrow in Fig. 3(a)]. These shape transformations occur without significant additional intermixing, suggesting that material is essentially redistributed within the island ensemble. Coarsening governs the evolution as long as shallow islands are present on the film. When all islands have barn shapes, intermixing becomes the only available strain-relaxation channel available. (Dislocation introduction during annealing is not observed, see below.) These results indicate that alloying during annealing, which requires Si diffusion from the substrate to the surface through the wetting layer, is slow compared to material redistribution among islands. The presence of barns, characterized by facets with a large contact angle with the substrate, may promote the outdiffusion of Si because of the large stress present at their base and surroundings. This simple model, which describes the shape oscillations by a "walk through the SiGe/Si(001) island phase diagram," is able to account for our experimental observations.

Surprisingly, for annealing times longer than 150 min, the average island volume does not increase as one would expect for continuous SiGe alloying but rather decreases. The same evolution is observed for the total volume per unit area contained in the islands (not shown here), indicating that some of the material composing the islands is re-deposited on the wetting layer. This phenomenon, which has already been observed during annealing of InP/GaAs(001) quantum dots,[25] can be qualitatively understood by considering that the critical thickness for the 2D-3D transition increases with decreasing misfit. This has been observed experimentally[26] and a similar behavior has been recently predicted theoretically.[27] We can speculate that an increased critical thickness will allow the transfer of material from the islands to the wetting layer, leaving shallower and Si-richer islands on the surface.

Finally, we also consider the morphological evolution of plastically-relaxed islands during extensive *in situ* annealing. Representative AFM scans ($1\ \mu m \times 1\ \mu m$) of dislocated islands contained in the as-grown sample and in the sample annealed for 360 min at 740 °C are shown in Figs. 4(a) and 4(c), respectively. A simple comparison shows that the *shape* of superdomes also changes during in situ annealing. Indeed, prior to annealing, dislocated islands exhibit a steep morphology [Fig. 4(a)],[11] while after 360 min annealing, their surface is mainly bounded by shallow {105} facets [Fig. 4(c)]. Nevertheless, dislocated islands can be distinguished from coherent islands because their *size* remains larger throughout the annealing process. These observations indicate that, during annealing, the residual strain present in dislocated islands is gradually relieved by intermixing and ripening as for coherent islands. For a superdome, the misfit strain prior to annealing is $\varepsilon=\varepsilon_0-nb/w$, where ε_0 is the misfit strain for a coherent island, n is the number of dislocations, b is the misfit component of the Burgers vector, and w is the mean island width.[28] Because of the reduced misfit, dislocated islands undergo transitions at critical volumes larger than for coherent islands. AFM scans of the *same* sample areas shown in Figs. 4(a) and 4(c) taken after selective wet chemical etching in a BPA solution are shown in Figs. 4(b) and 4(d), respectively. In the as-grown sample, the superdome leaves behind a complex footprint consisting of circular tree-ring structures[29] surrounding a central plateau.

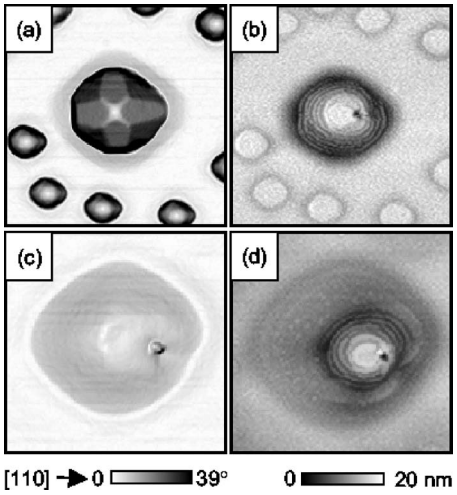

FIG. 4. (a) AFM scan (1 μm$\times$1 μm) of the same superdome contained in the as-grown sample prior to and (b) after 2 min etching in a BPA solution. The tree-ring structure is evident. (c) AFM scan (1 μm$\times$1 μm) of a large pyramid contained in the sample annealed for 360 min at 740 °C prior to and (d) after 2 min etching in a BPA solution. Similar tree-ring structures are observed but the island base area has considerably increased.

This particular structure was attributed to their cyclic growth mode.[28,29] After 360 min annealing, the islands base area becomes much larger [Fig. 4(d)] while the number of rings does not increase, suggesting that SiGe alloying and coarsening are always preferred to the introduction of additional dislocations throughout the annealing process. Tree-ring structures are clearly observed even for the sample annealed for 900 min, indicating that bulk-interdiffusion, which would smear the interface between island and substrate, does not play a significant role even at the relatively high temperature (740 °C) used here.

In conclusion, we observed that the island shape oscillates with the annealing time. This result is discussed using a simple model based on the dependence of the equilibrium island shape on both volume and composition. The evolution is driven by surface-mediated SiGe alloying when islands have a steep morphology, while it follows anomalous coarsening when different shapes are present. Dislocated islands evolve similarly to coherent islands, without introduction of additional dislocations throughout the annealing process. Since coarsening and alloying are general phenomena and take place also for other SK systems, it seems reasonable to believe that shape oscillations may also occur for other strained material combinations.

We acknowledge K. v. Klitzing for his continuous support, J. Tersoff for fruitful discussions, ESRF and HASYLAB for the provision of synchrotron radiation facilities and the staff of ID10B and BW2 for their assistance. This work was financially supported by the BMBF (03N8711) and the EC (Contracts No. 012150 and NMP4-CT-2004-500101 "SANDiE").

*Corresponding author. Electronic mail: m.stoffel@fkf.mpg.de

[1] A. Vailionis, B. Cho, G. Glass, P. Desjardins, D. G. Cahill, and J. E. Greene, Phys. Rev. Lett. **85**, 3672 (2000).
[2] J. Tersoff, B. J. Spencer, A. Rastelli, and H. von Känel, Phys. Rev. Lett. **89**, 196104 (2002).
[3] I. Goldfarb, Phys. Rev. Lett. **95**, 025501 (2005).
[4] G. Costantini *et al.*, Appl. Phys. Lett. **85**, 5673 (2004).
[5] U. Denker, A. Rastelli, M. Stoffel, J. Tersoff, G. Katsaros, G. Constantini, K. Kern, N. Y. Jin-Phillip, D. E. Jesson, and O. G. Schmidt, Phys. Rev. Lett. **94**, 216103 (2005).
[6] E. Sutter *et al.*, Appl. Phys. Lett. **84**, 2262 (2004).
[7] M. Stoffel, A. Rastelli, J. Tersoff, T. Merdzhanova, and O. G. Schmidt, Phys. Rev. B **74**, 155326 (2006).
[8] F. M. Ross *et al.*, Science **286**, 1931 (1999).
[9] A. Rastelli, M. Stoffel, J. Tersoff, G. S. Kar, and O. G. Schmidt, Phys. Rev. Lett. **95**, 026103 (2005).
[10] T. I. Kamins *et al.*, Appl. Phys. A: Mater. Sci. Process. **67**, 727 (1998).
[11] T. I. Kamins *et al.*, J. Appl. Phys. **85**, 1159 (1999).
[12] Y. T. Zhang and J. Drucker, J. Appl. Phys. **93**, 9583 (2003).
[13] T. K. Carns *et al.*, J. Electrochem. Soc. **142**, 1260 (1995).
[14] G. Katsaros *et al.*, Surf. Sci. **600**, 2608 (2006).
[15] J. Stangl *et al.*, Appl. Phys. Lett. **79**, 1474 (2001).
[16] J. Stangl, V. Holý, and G. Bauer, Rev. Mod. Phys. **76**, 725 (2004).
[17] T. J. Krzyzewski and T. Jones, J. Appl. Phys. **96**, 668 (2004).
[18] D. M. Schaadt *et al.*, J. Vac. Sci. Technol. B **24**, 2069 (2006).
[19] A. Raab and G. Springholz, Appl. Phys. Lett. **77**, 2991 (2000).
[20] R. Hull and E. A. Stach, "Strain accommodation and relief in GeSi/Si heteroepitaxy," in *Thin Film Heteroepitaxial Systems*, edited by W. K. Liu and M. B. Santos (World Scientific, Singapore, 1999).
[21] F. Tinjod and H. Mariette, Phys. Status Solidi B **241**, 550 (2004).
[22] W. Dorsch *et al.*, Appl. Phys. Lett. **72**, 179 (1998).
[23] J. A. Floro, E. Chason, L. B. Freund, R. D. Twesten, R. Q. Hwang, and G. A. Lucadamo, Phys. Rev. B **59**, 1990 (1999).
[24] M. De Seta *et al.*, J. Appl. Phys. **92**, 614 (2002).
[25] J. Johansson *et al.*, Appl. Surf. Sci. **134**, 47 (1998).
[26] P. M. Petroff and S. P. Denbaars, Superlattices Microstruct. **15**, 15 (1994).
[27] Y. Tu and J. Tersoff, Phys. Rev. Lett. **93**, 216101 (2004).
[28] F. K. LeGoues, M. C. Reuter, J. Tersoff, M. Hammar, and R. M. Tromp, Phys. Rev. Lett. **73**, 300 (1994).
[29] T. Merdzhanova, S. Kiravittaya, A. Rastelli, M. Stoffel, U. Denker, and O. G. Schmidt, Phys. Rev. Lett. **96**, 226103 (2006).